

Analysis of Thin-Walled Elements, with Ribbed Stiffeners, in the State of Post-Critical Deformations

Przemysław Mazurek¹

¹ The Faculty of Mechanical Engineering and Aeronautics, Rzeszów University of Technology, Al. Powstańców Warszawy 8, 35-959 Rzeszów, Poland

E-mail: pmazurek@prz.edu.pl

ABSTRACT

The paper presents the results of research on fragments of thin-walled coverings made of aluminum alloy. The examined structures were subjected to shear stresses leading to post-critical deformations. Three types of elements were analyzed: an element without stiffeners (the referencial one), an element with three stiffening ribs and an element with five stiffening ribs. The results of numerical analyzes and static experimental research were presented. Although this kind of solutions is commonly used in various aircraft structures, the publications about it are usually hard to rich [8, 9, 15]. The research concerning ribbed stiffeners are usually performed inside laboratories of aerospace concerns and their results are not published in the open sources. The general direction of analyses of this solution is indicated in presented study.

Keywords: numerical analysis, experimental tests, buckling, postbuckling.

INTRODUCTION

The aviation structures are a special case of mechanical structures. From the beginning of the aviation development, efforts were made to make them as strong and stiff as possible, while simultaneously reducing their weight. This resulted in a large variety of more or less successful structural solutions. In the initial period, generally accepted rules were used, which had been tested comprehensively in the design of other types of mechanical structures. Basing on the assumption that an airplane constructed in this way should only rise into the air, this kind of approach had often turned out to be sufficient. Over time, airplanes were assigned more and more serious tasks, which forced the search for solutions that allowed to minimize the weight of the load-bearing structure, and thus gave the opportunity to increase the disposable load and range. The use of aluminum alloys for the production of thin-walled structural elements made it possible to reduce their thickness, which, however, caused the problem of the lost stability.

The implementation of additional covering stiffenings eliminated such phenomena, unfortunately resulting in a simultaneous increase in weight, and thus reduced the profitability of air transport. Other solutions, such as: the use of grooved coverings or corrugated plate, enabled to exclude the states of post-critical deformations, however, at the cost of increased aerodynamic resistances, which in turn increased fuel consumption and significantly limited the ability to achieve higher speeds by an airplane. The constant striving to increase the speed imposed a change in the approach to the problem of designing thin-walled air coverings, allowing the appearance of a local loss of the covering panel's stability [10, 11, 12, 13]. It is subjected to additional conditions, according to which the covering may lose its stability only when this phenomenon occurs in the area limited by stiff elements of the framework and has an elastic nature.

Nonetheless, there is a group of elements, such as the wing spar walls and torsion box coverings, for which the loss of stability is unacceptable.

One of the methods of preventing the occurrence of post-critical deformations is the use of stiffening ribs [8, 9, 15]. The advantage of this type of solution is a significant increase in stiffness, while maintaining the same weight of structural elements. This solution is widely used both in the case of large communication aircrafts, in order to stiffen the internal parts of the load-bearing structure, as well as in the case of small sports and executive aircrafts, where apart from internal elements, such solutions are used to stiffen the panels of thin-walled coverings.

PURPOSE AND SCOPE OF THE RESEARCH

The paper presents the results of research on thin-walled structural elements, stiffened with ribs, in the states of post-critical deformations. (example – Fig. 1).

The aim of the research was to determine the increase in stiffness of elements with stiffening ribs in relation to the unstiffened element. The analyzes were based on experimental research performed on three types of elements with identical dimensions: an element without ribs, an element with three ribs and an element with five ribs. The form of deformation and the values of normal displacements to the surface were determined by using an optical scanner. The obtained results were used to generate adequate numerical models in the MSC Software environment. The conformity of the forms and the deformation values obtained numerically and experimentally enabled to

recognize the stress distributions as reliable, under the principle of equivalence of solutions, stating that a given form of deformation corresponds to one and only one type of stress distribution.

EXPERIMENTAL STUDIES

Experimental studies were conducted on three versions of the covering models, made of aluminum alloy 2024, with a thickness of 0.7 mm (Fig. 2). In both cases of stiffened structures, the same rib geometry was applied (Fig. 3).

The examined structures were attached with bolts to pinned steel beams of high stiffness. This enabled to subject them to pure shear. The right upper corner was anchored in the fixed support, while the left upper corner was fixed in the sliding support (Fig. 4b). The load was applied with a single-acting lever system, driven by the electro-mechanical actuator from Zwick - Roell (Fig. 4a).

The measurement of the reference points displacements and the form of deformation was carried out using the Atos optical 3D scanner from GOM (Fig. 5).

In all three cases, the maximum load was 9,000 N. The pictures obtained through scanning present a significantly different nature of post-critical deformations in individual cases.

In the case of the element without stiffeners, five folds appeared, with a large, dominant fold along the diagonal (Fig. 6a). This results in a strong flexural effect in a large part of the examined area. The element with three stiffeners

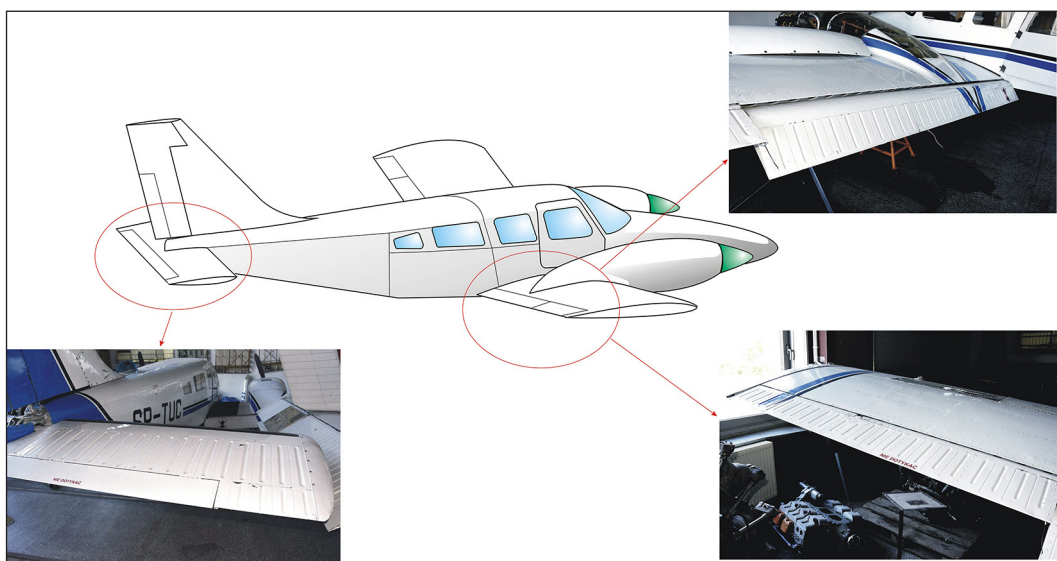


Fig. 1. Example of the application of coverings stiffened with ribs in an aircraft structure (PZL M-20 Mewa)

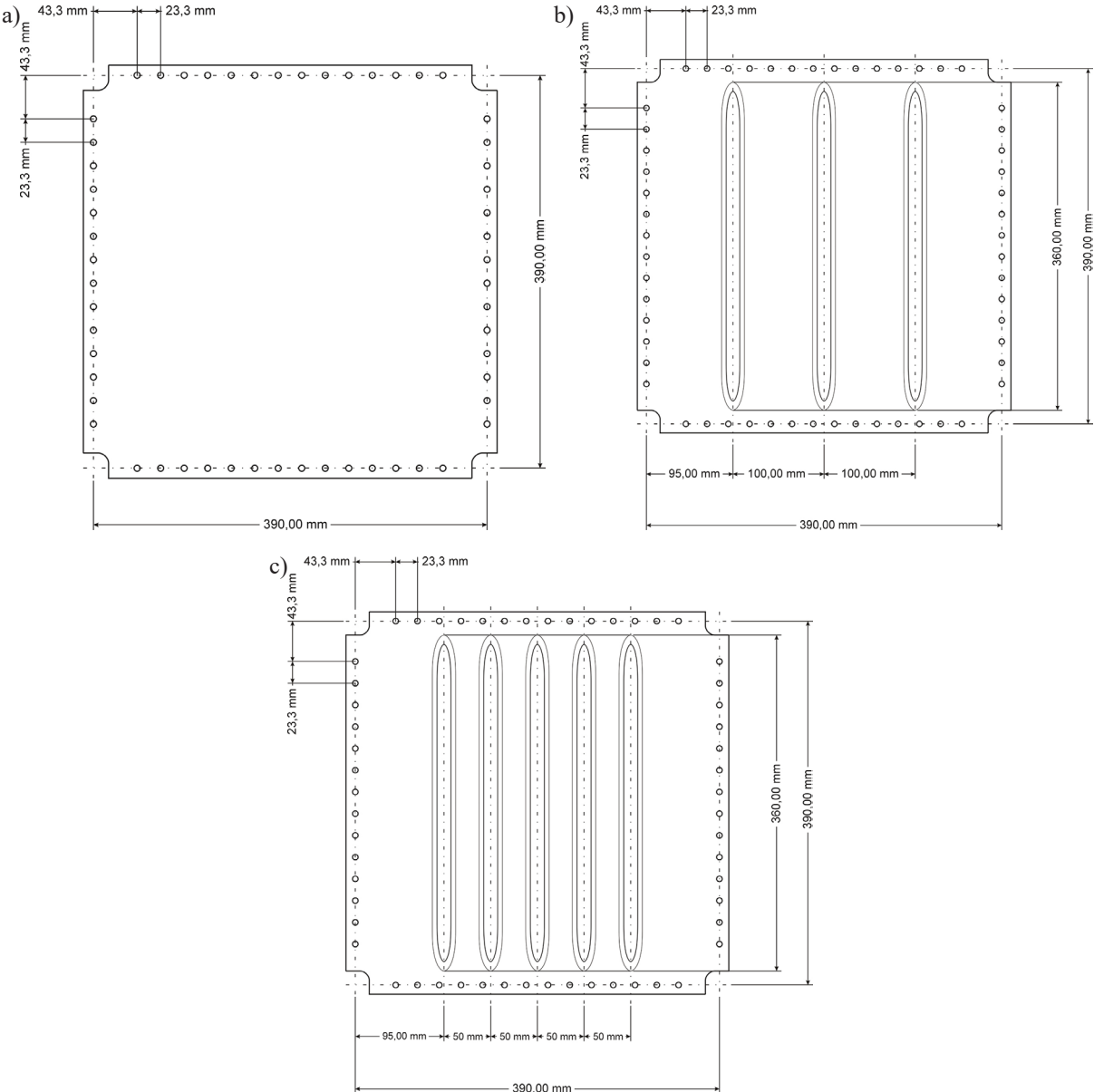


Fig. 2. Geometry of the analyzed models: (a) element without ribs, (b) element with three ribs, (c) element with five ribs

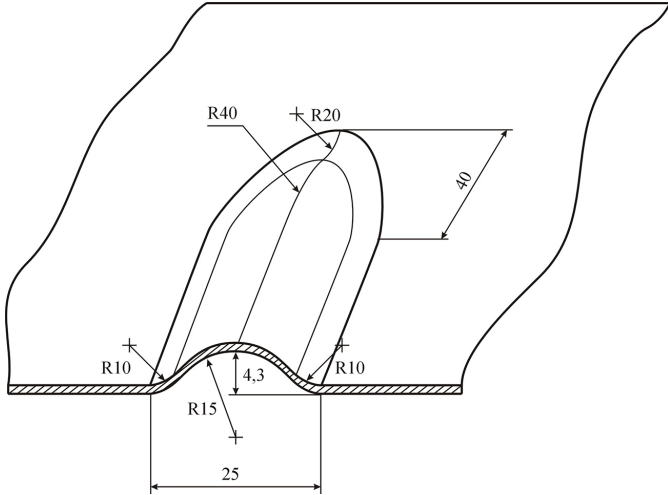


Fig. 3. Rib geometry

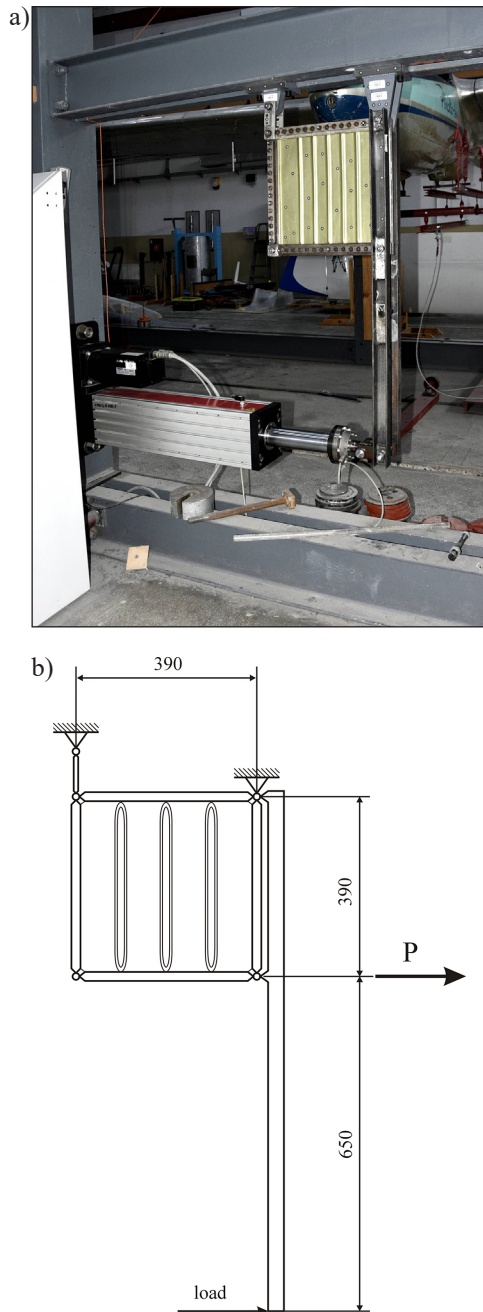


Fig. 4. (a) Test stand, (b) scheme of the loading system



Fig. 5. One of the examined elements together with the Atos 3D scanner

showed the appearance of four folds, including two dominant ones (Fig. 6b). And in the case of the element stiffened with five ribs, what appeared was an expansive, single deformation with a large radius of curvature and two much smaller deformations at the corners (Fig. 6c).

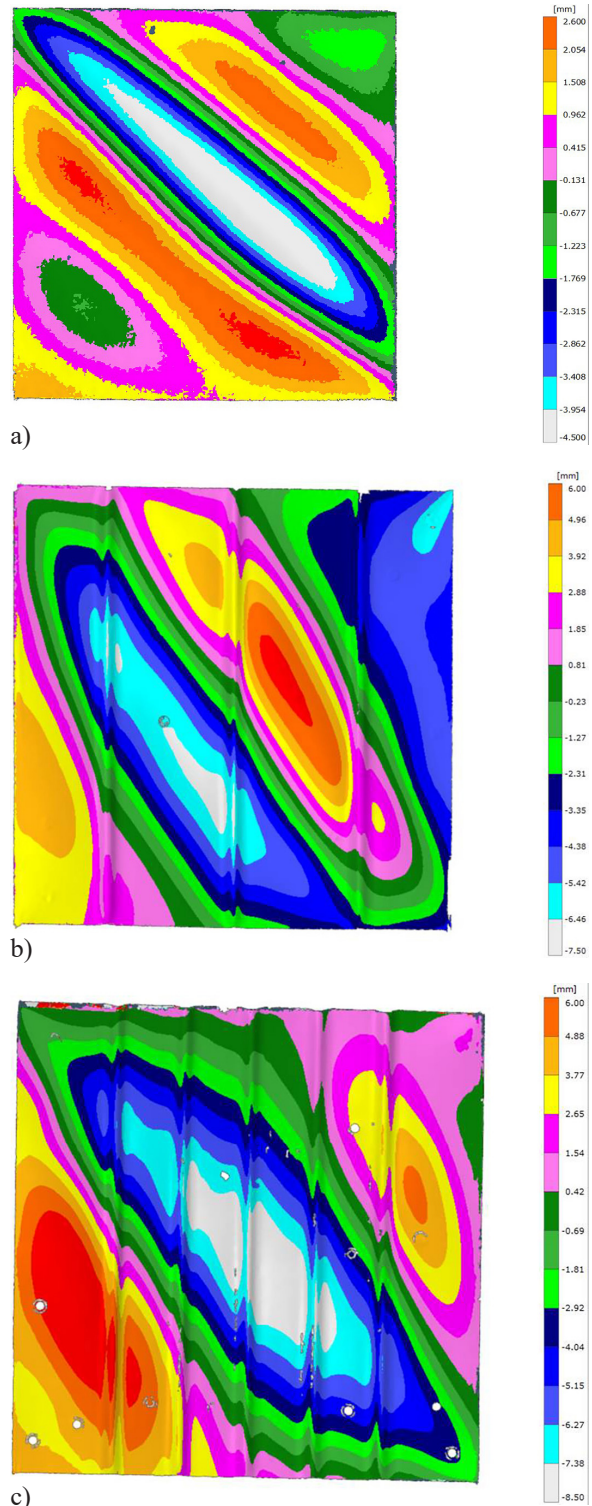


Fig. 6. Deformation fields obtained through 3D scanning: (a) element without stiffeners, (b) element with three ribs, (c) element with five stiffeners

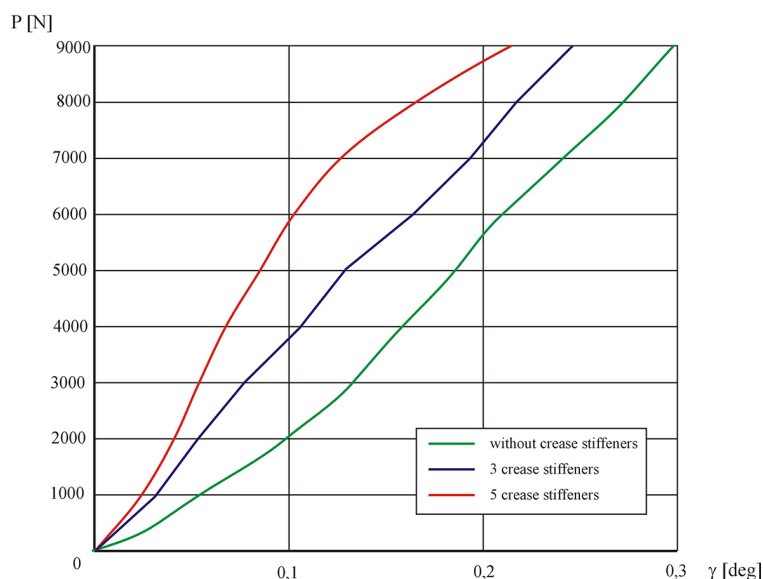


Fig. 7. Representative equilibrium paths obtained during experimental research

Measurement of the reference points displacements allowed for the determination of representative equilibrium paths, constituting the relations between the shear strain angle and the load value (Fig. 7).

The equilibrium path of the element without stiffeners for a low load range is marked by a relatively quick increase in deformations. This corresponds to the phase of folds formation and the increase in their curvature. After exceeding the value of approx. 3,000 N, the equilibrium path demonstrates an approximately constant pitch, which proclaims the stabilization of the character of losing stability and the formation of a tension field in the examined area, and thus stiffening of the structure. In the case of the element with three ribs, the diagram maintains an approximately constant pitch in the full load range. This confirms the different nature of the distribution of internal forces than in the first case. The structure with five ribs was marked by relatively high stiffness in the initial phase of the load increase. After the force of 7,000 N is exceeded, a decrease in stiffness is noticeable, caused by, as supposed, the development of post-critical deformations in a given distribution. Therefore, it should be stated that each of the examined structures was marked by a different nature of post-critical deformations distribution as well as a different course of their formation.

NUMERICAL ANALYSIS

On the grounds of the results obtained during the experimental research, it was possible to generate adequate numerical models using the

MSC Patran program, operating on the basis of the finite element method. Nonlinear numerical analyzes were conducted with the MSC MARC solver, using the Newton-Raphson method, with adaptive state control [1, 6, 7]. The results obtained through numerical calculations were compared with the results of the conducted experimental research, taking for the criterion the compatibility of the obtained deformation forms and of the courses of the equilibrium paths.

Numerical models of all three types of the examined systems were made on the basis of bilinear surface elements, preferred by the software maker for this type of analyses. Finite elements meshes were generated (Fig. 8), which included approximately 5,200 thin shell elements [14] and 5,400 nodes for the analyzed coverings fragments, and about 2,000 thick shell elements and 2,200 nodes for the stiff edges. In the case of the examined systems, numerical models were assigned a linearly resilient material model with parameters corresponding to the 2024 aluminum alloy ($E = 7.4 \cdot 10^4$ MPa, $\nu = 0.34$). For the stiff edges, the material model corresponding to steel was applied ($E = 2.1 \cdot 10^5$ MPa, $\nu = 0.3$).

As a result of the conducted calculations, contour images were obtained, presenting the values of displacements in the direction normal to the surface of the elements (Fig. 9).

The values of the displacements normal to the surface of the elements obtained with numerical calculations showed a satisfactory qualitative and quantitative compatibility with the corresponding values obtained during experimental research. In the case of the element without stiffeners, the

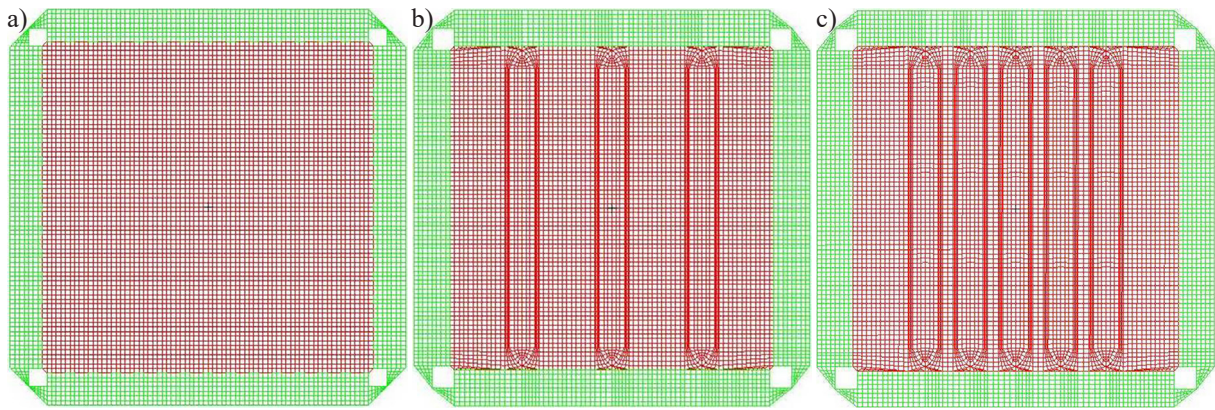


Fig. 8. Numerical models of the analyzed structures: (a) element without stiffeners, (b) element with three stiffeners, (c) element with five stiffeners

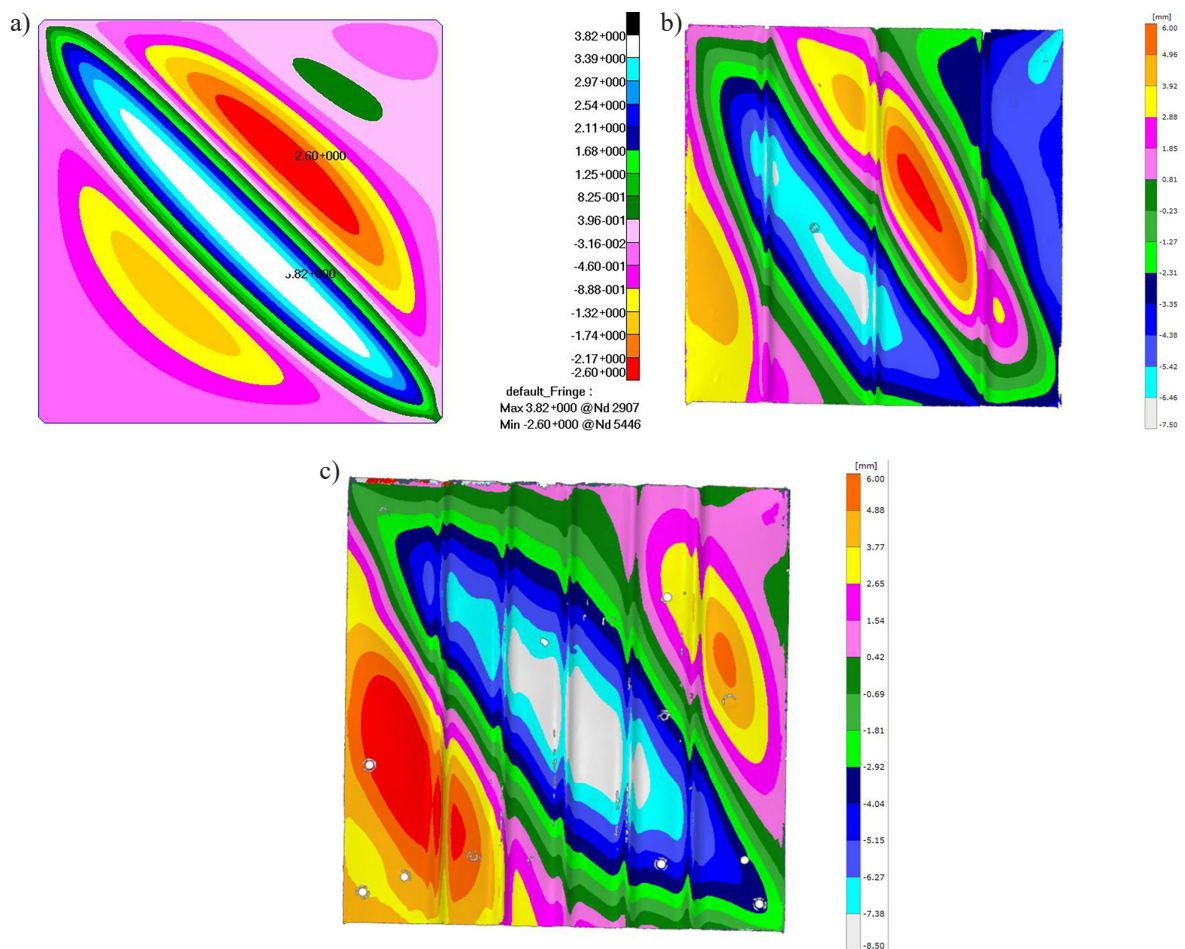


Fig. 9. Distribution of the displacements normal to the surface: (a) element without stiffeners, (b) element with three stiffeners, (c) element with five stiffeners

greatest discrepancy in results was obtained, coming to about 15% for the dominant fold. The differences obtained for the element with three ribs came to 7.3%. The smallest discrepancy between the calculations and the experiment (3.4%) was obtained for the element with five ribs.

The second criterion used to evaluate the accuracy of the conducted numerical analyzes was

the compliance of representative equilibrium paths, determining the value of the deformation angle in a function of the applied load (Fig. 10).

The comparison of representative equilibrium paths shows that the numerical models demonstrated slightly higher stiffness in comparison to the experimental structures. The reason for these discrepancies may be the idealized geometry of the

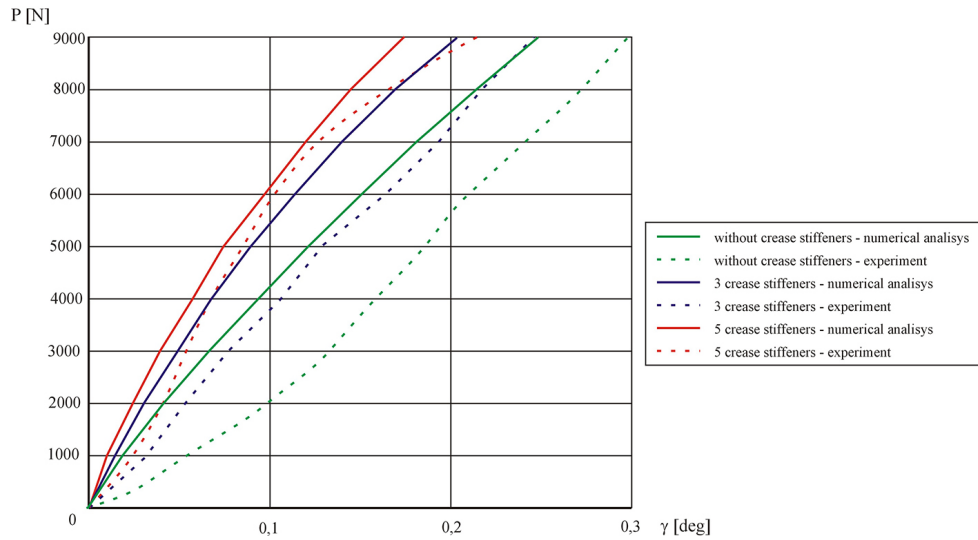


Fig. 10. Representative paths of equilibrium obtained through numerical analyses, related to the results of experimental research

Table 1. Differences between numerical analysis and experimental research

Element	Deformation angle			Max normal displacement		
	Experiment [deg]	Numerical analysis [deg]	Deviation [%]	Experiment [mm]	Numerical analysis [mm]	Deviation [%]
Without stiffeners	0.3	0.25	20	4.5	3.8	15.6
3 stiffeners	0.24	0.205	14.58	7.5	6.9	8
5 stiffeners	0.21	0.18	14	8.5	8.21	3.4

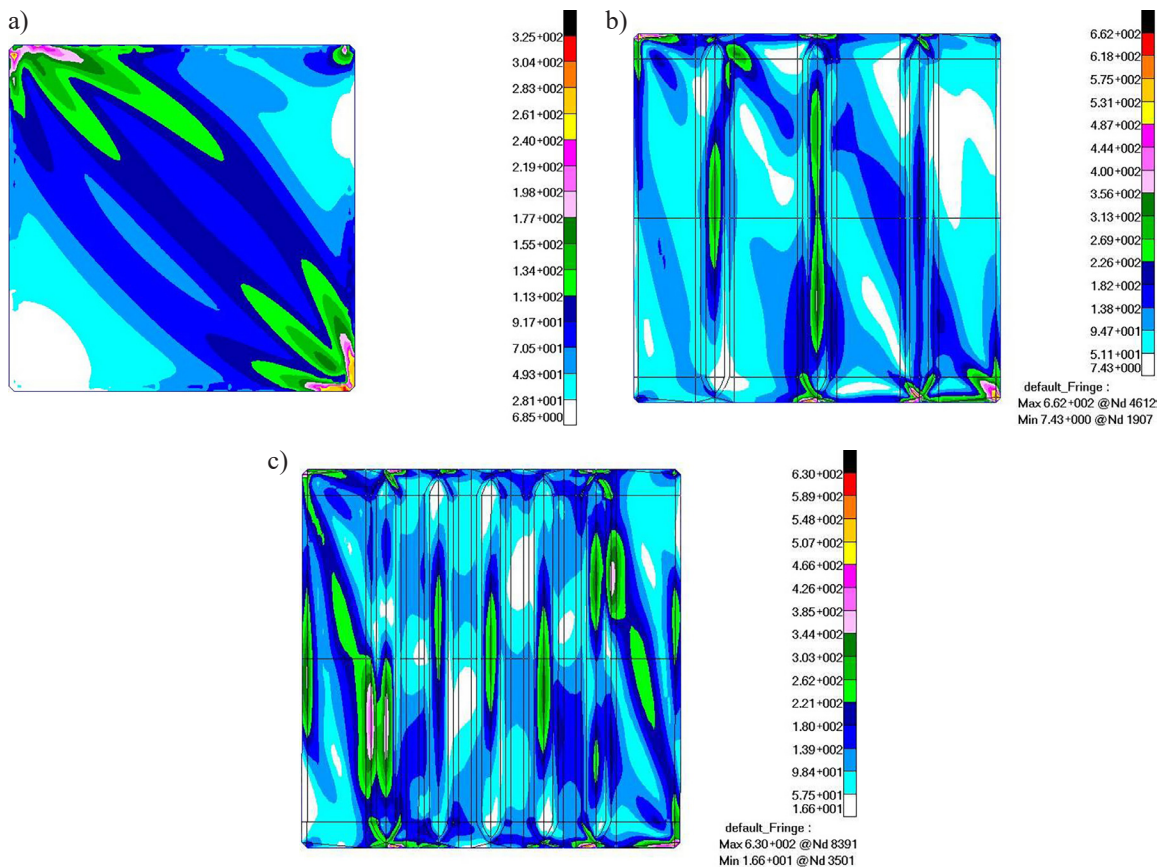


Fig. 11. Stress distribution according to the Huber-Misses-Hencky hypothesis: a) element without stiffeners, b) element with three stiffeners, c) element with five stiffeners



Fig. 12. Composite panel reinforced with “shaped” stiffeners

numerical models, devoid of any imperfections. Taking into account the possibility of measurement errors coming from a number of factors influencing the results of the experiment (such as backlashes between the stand elements, fixing imprecision, the possibility of slight displacements of the element in the stiff edges, etc.), it may be considered that the results of numerical calculations present a satisfactory consistency with experimental research. Differences between numerical analysis and experimental research are presented in Table 1.

Obtaining a satisfactory consistency of deformation fields and representative equilibrium paths allows for the assumption that numerical models are adequate equivalents of real objects. Therefore, it may be considered that the determined reduced stress distributions (Fig. 11) are of reliable nature and value.

The stress distribution images showed that in the case of the element without stiffeners, concentrations occur along three folds with high curvature and in the corners. The implementation of stiffening ribs significantly changed the stress distribution. In the element with three ribs, concentrations appear on the ridges of ribs, which arises from small radii of curvature on their ridges. Additionally, strong, local concentrations of a very high value are noticeable at the ends of ribs adjacent to the stiff framing. They result from sudden changes of stiffness, on the one hand from a sudden change in geometry, and on the other hand from the immediate vicinity of the stiff edges. A similar effect is also noticeable in the case of the element with five ribs. The appearance of such effects may raise serious concerns about the strength of the structure under both static loads and, above all, in the event of cyclically variable loads.

CONCLUSIONS

A comparative analysis of three versions of the examined thin-walled elements, mapping

fragments of the covering of aviation structures, leads to a number of observations, the most important of which seems to be the statement that, despite the use of identical boundary conditions and dimensions of the evaluated structures, the obtained forms of post-critical deformations had fundamentally different nature.

A significant increase in the stiffness of the structures reinforced in this way is noticeable. Concerning the reference object, in the case of stiffening with three ribs it was about 20% and in the case of five ribs – about 30%. It should be also noted that the improvement of the stiffness parameters was achieved without increasing the mass of the examined structures.

In the case of a smooth element, during the first phase of loading (up to 25% of the maximum value), a very rapid increase in the deformation angle was noted. This is an undesirable phenomenon due to the fact that the stiffness of the working covering of thin-walled structures essentially determines the torsional stiffness of the entire structure. An insufficient torsional stiffness of the structure, already present at low loads, may endanger the safety of the aircraft. After stabilization of the post-critical deformation state, the diagram becomes approximately linear, inclined at a much greater angle than in the initial phase.

The element with three ribs is marked by an approximately linear relationship of deformations in a function of shear stresses. Hence, this type of modification of the geometry enables to make the structure properly stiff and to maintain it in the entire range of the considered loads.

The course of the graph of the deformation angle's dependence on the operating load, obtained for the structure with five ribs, is disturbing. In the initial phase of loading, the angle increment is close to linear one, and the stiffness of the ribbed element is nearly twice as high as that of the smooth element. However, after reaching about 75% of the predicted maximum load value, the graph becomes curved, indicating a sudden loss of stiffness.

The representative equilibrium paths obtained through numerical calculations presented similar proportions of stiffness increase for individual solutions as in the case of the experiment, but they were of a more regular nature. This is due to the high degree of idealization of numerical models and the lack of possibility to recreate some imperfections of real objects. The differences between the results of the numerical analyses and obtained by means of experiment seem to be an effect of the lack of natural imperfections in the idealised virtual model. The less stiff connections of the

examined shell and the frame, result the reduction of the stiffness of all experimental model.

The results obtained through numerical calculations showed a very large influence of ribs, both on the nature of the stress distribution and their values. The unstiffened element showed a strong concentration of stresses along the diagonal in the direction of which the main fold appeared after the loss of stability. In the case of stiffened structures, stress concentrations appeared along the ridges of ribs. There were also small areas located between the end of the rib and the elements of the stiff framing, demonstrating strong local stress concentrations. This phenomenon forces a detailed analysis of the geometry of this type of stiffeners and a rational selection of both the ribs curvature radii and the distance of their ends from the stiff structural elements cooperating with the covering. A detailed inspection of the elements subjected to static experimental research did not reveal any damage of the material in this area. Therefore, it can be assumed that we are dealing with some kind of peculiarities of the numerical solution, arising from the lack of possibility to accurately recreate the conditions of the experiment during calculations.

Finally, it should be noted that this type of stiffening is intended to prevent any form of large deformation, in particular in the light load range, and not to improve the stress distribution in post-critical states. Therefore, it is necessary to select the geometrical parameters of the ribs in such a way that the covering does not lose its stability.

The results presented in this study suggest the need for further research aimed at determining the rational shape and size of the ribbed stiffeners.

The conducted research and numerical analyses present the usefulness of this type of stiffeners, considered not only in the context of their application in order to improve the performance parameters of metal structure elements, but also in application into composite structures [2, 3, 4, 5, 16]. In this case, the name of the reinforcement should be changed to, for example, “shaped” or “slat”, because the term “ribbed” will not be correct in this case. An example of this type of structural solution, in the form of a panel made of carbon-epoxy composite, is shown in Figure 12.

REFERENCES

1. Bathe K.J. Finite element procedures in engineering analysis. Prentice-Hall, Englewood Cliffs; 1982.
2. Debski H. Stability problems of compressed thin-walled structures. *Advances in Science and Technology-Research Journal*. 2018; 12(4), 190–198.
3. Debski H., Teter A. Numerical and experimental studies on the limit state of fibre-reinforced composite columns with a lipped channel section under quasi-static compression. *Composite Structures*. 2015; 133: 1–7.
4. Falkowicz K., Debski H. Postbuckling behaviour of laminated plates with a cut-out. *Advances in Science and Technology-Research Journal*. 2017; 11(1): 186–193.
5. Falkowicz K., Ferdynus M., Debski H. Numerical analysis of compressed plates with a cut-out operating in the geometrically nonlinear range. *Eksploracja i Niezawodnosc-Maintenance and Reliability*. 2015; 17(2), 222–227.
6. Felippa C.A. *Advanced finite element methods*, (ASEN 5367) Dept. of Aerospace Eng. Sci. Boulder, Colorado 2006.
7. Felippa C.A. *Nonlinear finite element methods*, (ASEN 5107) Dept. of Aerospace Eng. Sci. Boulder, Colorado, 2006.
8. Hosseini-Toudeshky H., Loughlan J., Kharazi M. The buckling characteristics of some integrally formed bead stiffened composite panels. *Thin-Walled Structures*. 2005; 43: 629–645.
9. Hosseini-Toudeshky H., Ovesy H.R., Kharazi M. The development of an approximate method for the design of bead-stiffened composite panels. *Thin-Walled Structures*. 2005; 43: 1663–1676.
10. Kopecki T. Numerical-experimental analysis of the post-buckling state of a multi-segment and multi-member thin-walled structure subjected to torsion. *Journal of theoretical and applied mechanics*. 2011; 49(1): 227–242.
11. Kopecki T. Numerical and experimental analysis of post-critical deformation states in a tensioned plate weakened by a crack. *Journal of Theoretical and Applied Mechanics*. 2010; 48(1): 45–70.
12. Kopecki T., Mazurek P. Determination of stress distribution patterns in post-critical deformation states of thin-walled skins subjected to operating loads. *Eksploracja i Niezawodnosc-Maintenance and Reliability*. 2014; 16(4): 608–615.
13. Kopecki T.; Świąch Ł. Experimental and numerical analysis of post-buckling deformation states of integrally stiffened thin-walled components of load-bearing aircraft structures. *Journal of Theoretical and Applied Mechanics*. 2014; 52(4): 905–915.
14. MSC Software : „MSC MARC 2017, User’s Guide”, MSC Software Corporation, 2016.
15. Słota J., Kubit A., Trzepieciński T., Krasowski B., Varga J. Ultimate load-carrying ability of rib-stiffened 2024-T3 and 7075-T6 aluminium alloy panels under axial compression. *Materials*. 2021; 14(1176): 1176.
16. Wymulski P., Debski H., Rozyło P., Falkowicz K. A study of stability and post-critical behaviour of thin-walled composite profiles under compression. *Eksploracja i Niezawodnosc-Maintenance and Reliability*. 2016; 18(4): 632–637.